Organic Electronics 81 (2020) 105671

Contents lists available at ScienceDirect

Organic Electronics

journal homepage: http://www.elsevier.com/locate/orgel

Tuning spin-orbit coupling towards enhancing photocurrent in hybrid organic-inorganic perovskites by using mixed organic cations

Yixuan Dou [a], Hengxing Xu [a], Yongtao Liu [a], Miaosheng Wang [a], Jia Zhang [a], Olga S. Ovchinnikova [b], Bin Hu [a,*]

[a] Department of Materials Science and Engineering, University of Tennessee, Knoxville, TN, 37996, USA
[b] Center for Nanophase Materials Sciences, Oak Ridge National Laboratory, Oak Ridge, TN, 37831, USA

ARTICLE INFO

Keywords:
Perovskites
Solar cells
Spin-orbit coupling
Organic cation
Photocurrent

ABSTRACT

The presence of the heavy elements leads to strong spin-orbit coupling (SOC) in hybrid organic-inorganic perovskites (HOIPs), which plays an important role in the photovoltaic performance of HOIPs by changing the populations between bright and dark states. The organic cation is a critical composition and affects SOC via the interaction with the inorganic cage. In this work, we use magneto-photocurrent measurement to explore the SOC effect upon using mixed organic cations (methylammonium (MA) and formamidinium (FA)) with different dipole moments in Pb based perovskites. Magneto-photocurrent measurements showed that the internal magnetic parameter B_0 is decreased from 402.41 mT to 180.18 mT and 104.58 mT with decreasing the MA/FA ratio. This provides evidence that changing the internal dipole moment by using mixed organic cations can essentially change the SOC in HOIPs. Simultaneously, the photocurrent is increased from 21.46 mA/cm^2 to 22.60 mA/cm^2 and 23.08 mA/cm^2 when the MA/FA ratio is changed from 1:0 to 0.9:0.1 and 0.7:0.3. Above all, our results indicate that the change in SOC by different organic cations can also be a factor affecting the performance of perovskite solar cells.

1. Introduction

Hybrid organic-inorganic perovskites (HOIPs) have emerged as a groundbreaking material for photovoltaic devices, light-emitting diodes, and lasers [1–4]. HOIP solar cells have achieved a high sunlight to electricity power conversion efficiency (PCE) of 25.2% in less than ten years, achieving the highest efficiency of thin-film solar cells, and comparable to currently commercialized solar cells in market [5]. Great efforts have been implemented to further improve the performance of HOIPs, and have a better understanding of the fundamental properties will point a more effective way for device optimization [6–10].

HOIP with outstanding photovoltaic property typically composed of ABX_3 structure (A = methylammonium, formamidinium, Cs; B = Pb^{2+}, Sn^{2+}; X = I^-, Br^-, Cl^-) [11,12]. The presence of relatively heavy elements (Pb^{2+} and I^-) in HOIPs lead to significant spin-orbit coupling (SOC) [13], which plays an important role on exciton population change between bright and dark states that are critical to the photovoltaic processes in HOIP solar cells [14–16]. Since the electronic structure of HOIPs is dominated by $[BX_6]^{3-}$ inorganic cages [17,18], most previous researches have studied the effects of B site metal cations and X site halide on SOC [19–21]. However, A site organic cation is also of prime importance because its motion affects the inorganic cage [16,22,23]. To date, extensive efforts have focused on the effects of A site cation, such as its effects on bandgap, stability, trap density, and ultimately PCE. However, rare research has shed light on its role in SOC of HOIPs, which is also critical to photovoltaice action.

In this work, we studied the role of A-site organic cation in SOC and hence photovoltaic actions in $MA_xFA_{(1-x)}PbI_3(Cl)$ solar cells by using mixed cation MA and FA with different dipole moment. A series of solar cells based on $MA_xFA_{(1-x)}PbI_3(Cl)$ were investigated by magneto-photocurrent measurement to explore the SOC and its effects on the photovoltaic performance of HOIP solar cells. Our results show decreased internal magnetic parameter B_0 value of $MAPbI_3(Cl)$, $MA_{0.9}FA_{0.1}PbI_3(Cl)$, and $MA_{0.7}FA_{0.3}PbI_3(Cl)$ is 402.41 mT, 180.18 mT, 104.58 mT, respectively, indicating the decrease of SOC with the decrease of MA/FA ratio. Meanwhile, the photocurrent increased from is increased from 21.46 mA/cm^2 to 22.60 mA/cm^2 and 23.08 mA/cm^2 with the decrease of MA/FA ratio, suggesting that the change in SOC

* Corresponding author.
E-mail address: bhu@utk.edu (B. Hu).

https://doi.org/10.1016/j.orgel.2020.105671
Received 22 November 2019; Received in revised form 9 January 2020; Accepted 15 January 2020
Available online 27 February 2020

induced by A-site cation substitution is critical to the photovoltaic performance of HOIP solar cells.

2. Results and discussion

We fabricated HOIP solar cells with an inverted (p-i-n) structure of ITO/NiO_X/$MA_xFA_{(1-x)}PbI_3$(Cl)/PCBM/PEI/Ag (Fig. 1) in this study, the fabrication method is described in Methods Session. Chlorine (Cl) was doped to passivate defects near grain boundaries in all HOIP films so as to improve the performance of solar cells. The current-voltage (J-V) characteristics of $MA_xFA_{(1-x)}PbI_3$(Cl)solar cells with different MA/FA ratio are shown in Fig. 1b. Table 1 summarizes the corresponding photovoltaic parameters including short circuit current (J_{sc}), open circuit voltage (V_{oc}), fill factor (FF), and PCE. It can be observed that MA/FA ratio decreasing leads to PCE enhancement. Fig. 1b–d present the change tendency of V_{oc}, J_{sc}, and FF, respectively, where the V_{oc} and the FF showed negligible change with MA/FA ratio changes. However, the J_{sc} increases obviously with MA/FA ratio decreases, which suggests that the PCE enhancement originates from J_{sc} changes.

To understand the origin of the J_{sc} enhancement, we investigated the absorption spectrum change of $MA_xFA_{(1-x)}PbI_3$(Cl) films upon the change of MA/FA ratio. Absorption is critical to the photocurrent of solar cells, stronger absorption allows more photons to convert to excitons and charges, resulting in higher photocurrent [24]. Fig. 2 shows the absorption spectra of three HOIPs, where we can observe that the three HOIPs show similar bandgap. Unexpectedly, although $MA_{0.7}FA_{0.3}PbI_3$(Cl) has lower absorption than $MAPbI_3$(Cl) and $MA_{0.9}FA_{0.1}PbI_3$(Cl), it shows the highest photocurrent. Therefore, the absorption change is not the origin of the J_{sc} and PCE enhancement of HOIP solar cells with different MA/FA ratios.

Morphology of three HOIP films is also investigated since grain size, grain boundary, and pinhole also affect the photovoltaic performance of HOIP solar cells [25]. Fig. 3 shows the scanning electron microscopy (SEM) images of three HOIPs thin films. However, SEM images indicate the morphology of three HOIPs thin films is very similar, all exhibit similar grain size and grain boundary and are pinhole free.

We further studied the trap density in three HOIP thin films by measuring J_{sc} as a function of illumination intensity and excitation-dependent photoluminescence (PL). The relationship of the J_{sc} and the illumination intensity(I) can be described using the equation: $J_{sc} \propto I^{\alpha}$ [26,27]. Devices with trap-assisted monomolecular recombination process shows an α value close to 1, the pure bimolecular recombination process shows a lower α value of 0.5. Therefore, α value suggests the significance of trap-assisted recombination in HOIPs [28,29]. Fig. 4a shows J_{sc} as a function of illumination intensity, where the illumination intensity varies from 10 mW/cm^2 to 100 mW/cm^2 and is on a logarithmic scale. The α values of all three HOIP solar cells are around 0.94, indicating that all three HOIPs have similar trap density. We further studied the relationship of illumination intensity and PL intensity is affected by traps inside perovskite films [30]. The PL intensity (I) and laser intensity have a relationship: PL $\propto I^{\alpha}$, $\alpha \sim 1$ implies an exciton-like transition and $\alpha < 1$ indicates defects or impurities evolved recombination way. As shown in Fig. 4b, all three HOIP solar cells show similar α values around 1, with only minor variation. These indicate that the variation in the photoelectronic process among our three HOIP films are not dominated by the difference in trap density, so does the difference in J_{sc}.

Table 1
Photovoltaic Parameter of $MAxFA_{(1-x)}PbI_3$ solar cells.

Sample name	J_{sc}	V_{oc}	FF	PCE%
$MAPbI_3$	21.4594	1.1097	0.6926	16.2839
$MA_{0.9}FA_{0.1}PbI_3$	22.6021	1.1021	0.6785	16.9014
$MA_{0.7}FA_{0.3}PbI_3$	23.0784	1.1021	0.7096	18.0489

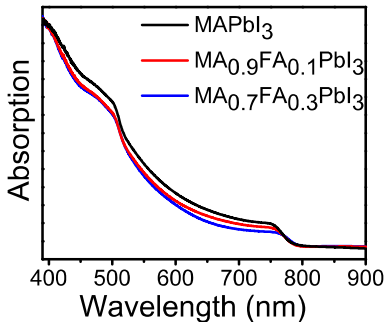

Fig. 2. Absorption spectra of $MAxFA_{(1-x)}PbI_3$ film.

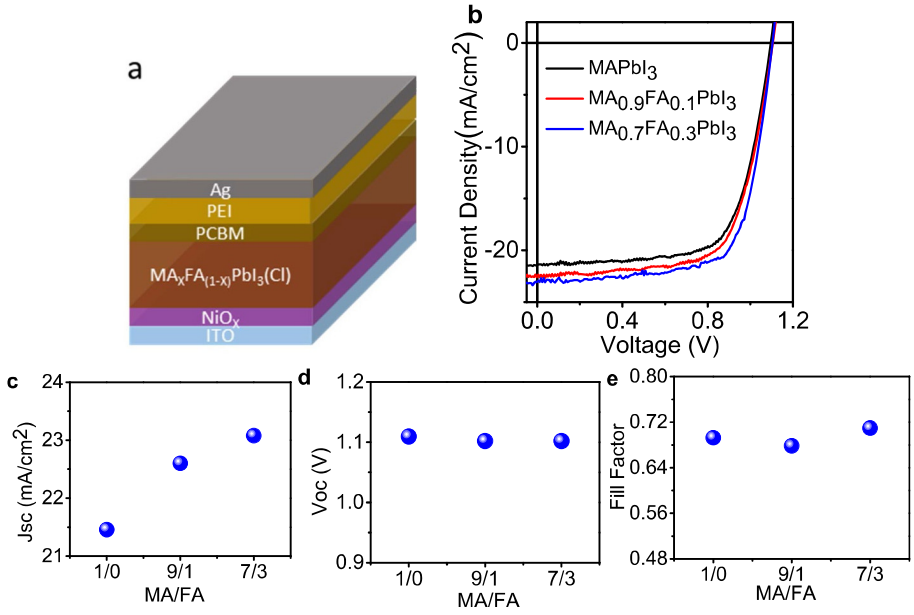

Fig. 1. a) Schematic diagram of perovskite solar cells. b) J−V characteristics of $MAxFA_{(1-x)}PbI_3$(Cl) solar cells. c-e) changes in Voc, Jsc, fill factor of $MAxFA_{(1-x)}PbI_3$(Cl) solar cells with changes in MA to FA ratio, respectively.

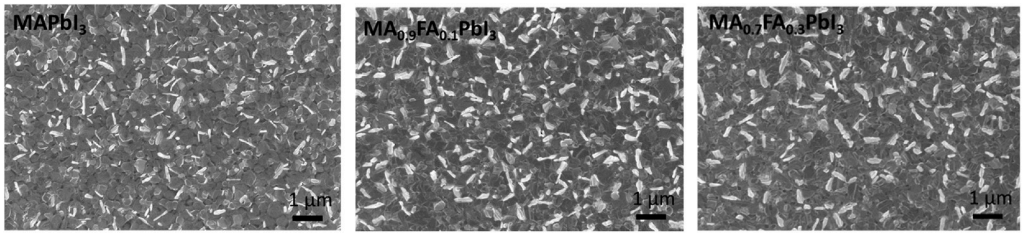

Fig. 3. Top-view SEM image of the of $MAxFA_{(1-x)}PbI_3$ HOIP film.

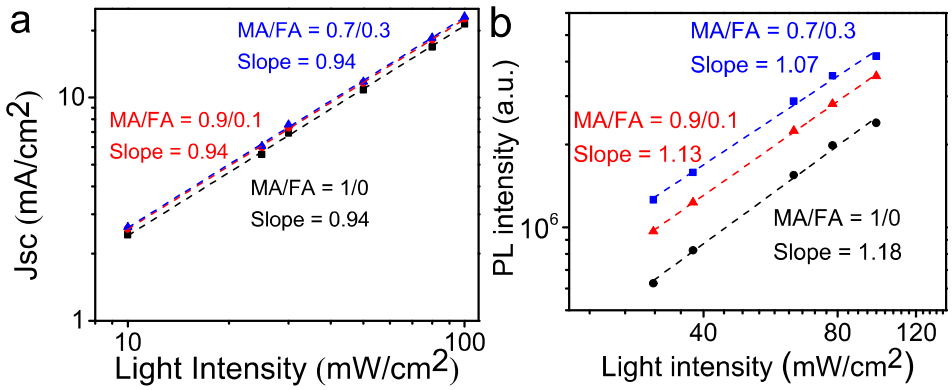

Fig. 4. a) Jsc of $MA_xFA_{(1-x)}PbI_3(Cl)$ solar cells plotted against light intensity on a logarithmic scale, b)PL of $MA_xFA_{(1-x)}PbI_3(Cl)$ plotted against laser intensity on a logarithmic scale.

Next, we consider the possibility that change organic cation can affect SOC, consequently change the population between bright and dark states. The magneto-J_{sc} measurement was used to monitor the SOC change of three HOIPs with different MA/FA ratios. Under illumination, photoexcitation quickly generates free carriers within 1 ps, free carriers have the opportunity to recombine to bright and dark states [31]. Spin mixing induced by SOC can lead to the conversion from dark to bright state, spin conserving due to exchange interaction tends to prevent the conversion between bright and dark states. The populations on the two states reach equilibrium due to the competition between spin mixing and spin conserving. After applying a magnetic field, the magnetic field would introduce coherent spin procession to the excited states, which leads to the increase of dark states. Thus, the conversion from dark state to bright state will be suppressed [32]. Since drak state is easier to be separated to generate photocurrent than bright state, the suppression of the conversion from dark state to bright state will lead to a positive magneto-J_{sc} signal. Fig. 5 shows positive magneto-J_{sc} signals are generated under magnetic field in both three HOIP solar cells, indicating the suppression of dark state to bright state conversion. It can also be observed in Fig. 5 that the curve shape of the magneto-Jsc is different among the three HOIP solar cells. The curve shape of the magneto-Jsc can be explicitly defined as the changing rate on the bright states/-dark states ratio caused by magnetic field. The changing rate of the bright/dark states is affected by the competition between magnetic field and spin mixing induced by SOC. Thus, with a stronger SOC, it is more difficult to change the populations between bright and dark states by an external magnetic field, leading to a broader line-shape in magneto-Jsc characteristics [19,33]. Fig. 5 indicates that the magneto-Jsc showed a narrower signal with the decrease of MA/FA ratio, suggesting stronger SOC in higher MA/FA ratio HOIP solar cells. By using non-Lorentz equation to fit the line-shape of magneto-Jsc, we can determine that the internal magnetic parameter B_0 related to SOC. The B_0 value of $MAPbI_3(Cl)$, $MA_{0.9}FA_{0.1}PbI_3(Cl)$, and $MA_{0.7}FA_{0.3}PbI_3(Cl)$ is 402.41 mT, 180.18 mT, 104.58 mT, respectively, further supporting that HOIPs with larger MA/FA ratio exhibit stronger SOC, corresponding to smaller photocurrent.

We also compare the PL lifetime of the three HOIP thin films using time-resolved photoluminescence (TRPL) measurement. Fig. 6 indicates a little lifetime difference can be observed among the HOIPs with different MA/FA ratios. By fitting the TRPL curve, we obtained the PL lifetimes of $MAPbI_3(Cl)$, $MA_{0.9}FA_{0.1}PbI_3(Cl)$, and $MA_{0.7}FA_{0.3}PbI_3(Cl)$, which are 61.20 ns, 71.91 ns, 81.89 ns, respectively, as shown in Table 2. According to our trap-density studies (Fig. 4) and SOC study (Fig. 5), this difference in PL lifetime of our three HOIP films can be induced by SOC difference. Dark and bright states can have longer and shorter lifetime because of longer and shorter forbidden transition,

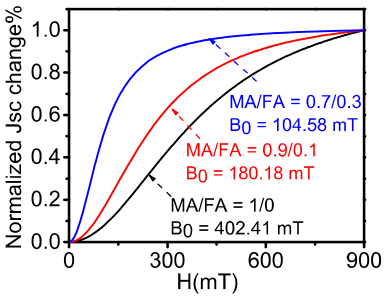

Fig. 5. Normalized magneto-photocurrent of $MA_xFA_{(1-x)}PbI_3(Cl)$ solar cells.

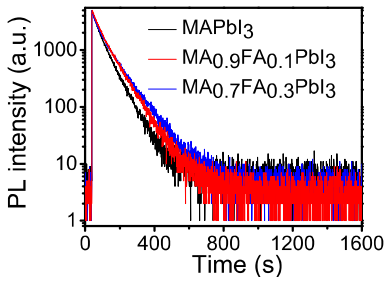

Fig. 6. TRPL spectra of the of $MAxFA_{(1-x)}PbI_3$ HOIP film.

Table 2
Lifetime of $MA_xFA_{(1-x)}PbI_3$ perovskite films.

Sample name	Lifetime (ns)
$MAPbI_3$	61.20
$MA_{0.9}FA_{0.1}PbI_3$	71.91
$MA_{0.7}FA_{0.3}PbI_3$	81.89

respectively. Thus the longer lifetime in HOIPs with increased MA/FA ratio could result from less bright states induced by the SOC decrease.

3. Conclusion

In summary, our results show that the SOC of HOIP altered by changing A site organic cation is also an important factor in additon to bandgap, trap density, stability that can impact the performance of HOIP solar cells. Our magneto-photocurrent measurements show decrease internal magnetic parameter B_0 value with MA/FA ratio decrease, suggesting that the SOC decreases with a smaller MA/FA ratio. Furthermore, the decrease of SOC induced by MA/FA ratio change leads to photocurrent and PCE enhancement of HOIP solar. Our work provides an effective approach to improve the performance of HOIP solar cells, which will be useful for further development of HOIP photovoltaic devices.

4. Experimental section

Materials: Lead(II) iodide (PbI_2, ultra-dry, 99.999%, metals basis), Nickel(II) formate dehydrate, and Ethylene glycol (99%) were purchased from Alfa Aesar; Methylammonium iodide (MAI) and formamidinium iodide (FAI) was purchased from Greatcell Solar Limited; Phenyl-C61-butyric acid methyl ester ($PC_{61}BM$) were purchased from 1-Material; Lead(II) chloride, γ-butyrolactone (GBL), toluene, dimethyl sulfoxide (DMSO), chlorobenzene, polyethylenimine (PEI, Mw~2000, 50 wt% in water), and isopropanol were purchased from Sigma-Aldrich. All materials were used as received.

Device Fabrication: The $MAPbI_3(Cl)/FAPbI_3(Cl)$ precursor solutions were prepared by dissolving MAI/FAI, $PbCl_2$ and PbI_2 with concentration of 1.2 M, 0.14 M and 1.26 M in a mixed solvent of γ-butyrolactone (GBL) and dimethyl sulfoxide (DMSO) (7:3 v/v), then mixing the two solution with volume ratio of 1:0, 9:1, 7:3 to get $MAPbI_3(Cl)$, $MA_{0.9}FA_{0.1}PbI_3(Cl)$ and $MA_{0.7}FA_{0.3}Pb\ I_3(Cl)$ solutions. All HOIP solar cells used in this work were fabricated with a planar structure of ITO/NiO_x/$MA_xFA_{(1-x)}PbI_3(Cl)$/PCBM/PEI/Ag. The NiO_x precursor solution was prepared by adding 0.5 M Nickel(II) formate dehydrate, 1 M equivalents of ethylenediamine in ethylene glycol, then the NiO_x layer was spin-cast on the top of precleaned indium tin oxide (ITO) substrates at 4000 rpm for 90 s, and subsequently annealed at 300 °C for 1 h in ambient conditions. The $MA_xFA_{(1-x)}Pb\ I_3(Cl)$ HOIP layers were spin-cast on top of NiO_x with a two-step spin coating process (1000 rpm for 10 s and 4000 rpm for 60 s), 400 μL toluene was dropped as antisolvent at the 20th second of the second step, then the $MAPbI_3(Cl)/MA_xFA_{(1-x)}PbI_3(Cl)$ film were annealed at 100 °C for 10 min. After cooling down, the $PC_{61}BM$(20 mg/mL) solution of Chlorobenzene was spin-coated on top of perovskite layer at 2000 rpm for 60 s. After 40 min, the 0.5 mg/mL PEI (Mw~2000, 50 wt% in water) solution in isopropanol was then spin-cast on top of $PC_{61}BM$ at 5000 rpm for 60 s. At the end, 90 nm silver layer was thermally deposited. In addition, all devices were encapsulated by glass covers with epoxy inside the glove box while taking measurements in ambient condition.

Characterization of photovoltaic performance: Current density-voltage (*JV*) characteristics were measured at 100 mW/cm^2 using solar simulator (Thermal Oriel 96000 300 W from Newport) and Keithley 2612 source meter in the nitrogen gas filled glovebox. For intensity-dependent Jsc measurement, neutral density filters were used to adjust the excitation intensities. Absorption were measured under UV/VIS spectrometer (Lambda 35, PerkinElmer). The magneto-photocurrent measurements were performed under an external magnetic field (B) parallel to the device plane scanning from 0 to 900 mT. For magneto-photocurrent, the photocurrent of perovskite solar cells at was recorded at a 0 V given bias at the same time, the incident light was from a 488 nm CW laser. The SEM image was acquired on a Zeiss Merlin scanning electron microscope.

Declaration of competing interest

The authors declare that they have no known competing financial interests or personal relationships that could have appeared to influence the work reported in this paper.

Acknowledgements

This research was supported by the financial supports from Air Force Office of Scientific Research (AFOSR) under the grant number FA 9550-15-1-0064, AOARD (FA2386-15-1-4104), and National Science Foundation (NSF-1911659). This research was partially conducted at the Center for Nanophase Materials Sciences based on user projects (CNMS2016-279, CNMS2016-R45, CNMS-2019-057), which is a U.S. Department of Energy Office of Science User Facility. The author (Y-X Dou) acknowledges the financial support from the China Scholarship Council through university agreement for her Ph.D study at the University of Tennessee (Knoxville).

References

[1] K. Lin, J. Xing, L.N. Quan, F.P.G. de Arquer, X. Gong, J. Lu, L. Xie, W. Zhao, D. Zhang, C. Yan, W. Li, X. Liu, Y. Lu, J. Kirman, E.H. Sargent, Q. Xiong, Z. Wei, Nature 562 (7726) (2018) 245–248.
[2] K. Kang, H. Ahn, Y. Song, W. Lee, J. Kim, Y. Kim, D. Yoo, T. Lee, Adv. Mater. 31 (21) (2019) e1804841.
[3] G. Li, T. Che, X. Ji, S. Liu, Y. Hao, Y. Cui, S. Liu, Adv. Funct. Mater. 29 (2) (2019) 1805553.
[4] E.H. Jung, N.J. Jeon, E.Y. Park, C.S. Moon, T.J. Shin, T.Y. Yang, J.H. Noh, J. Seo, Nature 567 (7749) (2019) 511–515.
[5] Research cell efficiency records. http://www.nrel.gov/ncpv (National Renewable Energy Laboratory).
[6] J. Chen, N.G. Park, Adv. Mater. (2018) e1803019.
[7] P. Cui, D. Wei, J. Ji, H. Huang, E. Jia, S. Dou, T. Wang, W. Wang, M. Li, Nat. Energy 4 (2) (2019) 150–159.
[8] L.V. Pilar, J. A, J. T, G.R. Manuel, R. Sandheep, G.B. Germà, B. Juan, A. Osbel, Adv. Energy Mater. 8 (14) (2018) 1702772.
[9] M. Saliba, J.-P. Correa-Baena, C.M. Wolff, M. Stolterfoht, N. Phung, S. Albrecht, D. Neher, A. Abate, Chem. Mater. (2018).
[10] W. Chen, Y. Zhou, G. Chen, Y. Wu, B. Tu, F.Z. Liu, L. Huang, A.M.C. Ng, A. B. Djurišić, Z. He, Adv. Energy Mater. 9 (19) (2019).
[11] J. Breternitz, S. Schorr, Advanced Energy Materials, 2018.
[12] Y. Fu, H. Zhu, J. Chen, M.P. Hautzinger, X.Y. Zhu, S. Jin, Nat. Rev. Mater. (2019).
[13] F. Zheng, L.Z. Tan, S. Liu, A.M. Rappe, Nano Lett. 15 (12) (2015) 7794–7800.
[14] H. Xu, M. Wang, Z.-G. Yu, K. Wang, B. Hu, Adv. Phys. 68 (2) (2019) 49–121.
[15] K. Liao, X. Hu, Y. Cheng, Z. Yu, Y. Xue, Y. Chen, Q. Gong, Advanced Optical Materials, 2019.
[16] A. Amat, E. Mosconi, E. Ronca, C. Quarti, P. Umari, M.K. Nazeeruddin, M. Gratzel, F. De Angelis, Nano Lett. 14 (6) (2014) 3608–3616.
[17] D.J. Kubicki, D. Prochowicz, A. Hofstetter, P. Pechy, S.M. Zakeeruddin, M. Gratzel, L. Emsley, J. Am. Chem. Soc. 139 (29) (2017) 10055–10061.
[18] J. Gebhardt, A.M. Rappe, Adv. Mater. (2018) e1802697.
[19] J. Zhang, T. Wu, J. Duan, M. Ahmadi, F. Jiang, Y. Zhou, B. Hu, Nanomater. Energy 38 (2017) 297–303.
[20] J. Even, L. Pedesseau, J.-M. Jancu, C. Katan, J. Phys. Chem. Lett. 4 (17) (2013) 2999–3005.
[21] J. Im, C.C. Stoumpos, H. Jin, A.J. Freeman, M.G. Kanatzidis, J. Phys. Chem. Lett. 6 (17) (2015) 3503–3509.
[22] D. Giovanni, H. Ma, J. Chua, M. Gratzel, R. Ramesh, S. Mhaisalkar, N. Mathews, T. C. Sum, Nano Lett. 15 (3) (2015) 1553–1558.
[23] A.M. Leguy, J.M. Frost, A.P. McMahon, V.G. Sakai, W. Kochelmann, C. Law, X. Li, F. Foglia, A. Walsh, B.C. O'Regan, J. Nelson, J.T. Cabral, P.R. Barnes, Nat. Commun. 6 (2015) 7124.
[24] D.P. McMeekin, G. Sadoughi, W. Rehman, G.E. Eperon, M. Saliba, M.T. Hörantner, A. Haghighirad, N. Sakai, L. Korte, B. Rech, M.B. Johnston, L.M. Herz, H.J. Snaith, Science 351 (6269) (2016) 151–155.
[25] T.S. Sherkar, C. Momblona, L. Gil-Escrig, J. Avila, M. Sessolo, H.J. Bolink, L.J. A. Koster, ACS Energy Lett 2 (5) (2017) 1214–1222.

[26] D. Bi, W. Tress, M.I. Dar, P. Gao, J. Luo, C. Renevier, K. Schenk, A. Abate, F. Giordano, J.-P. Correa Baena, J.-D. Decoppet, S.M. Zakeeruddin, M. K. Nazeeruddin, M. Grätzel, A. Hagfeldt, Sci. Adv. 2 (1) (2016) e1501170.
[27] V.D. Mihailetchi, J. Wildeman, P.W.M. Blom, Phys. Rev. Lett. 94 (12) (2005) 4.
[28] I. Riedel, J. Parisi, V. Dyakonov, L. Lutsen, D. Vanderzande, J.C. Hummelen, Adv. Funct. Mater. 14 (1) (2004) 38–44.
[29] M. Kuik, L.J. Koster, G.A. Wetzelaer, P.W. Blom, Phys. Rev. Lett. 107 (25) (2011) 256805.
[30] Y. Yamada, T. Nakamura, M. Endo, A. Wakamiya, Y. Kanemitsu, J. Am. Chem. Soc. 136 (33) (2014) 11610–11613.
[31] Y. Zhai, C.X. Sheng, C. Zhang, Z.V. Vardeny, Adv. Funct. Mater. 26 (10) (2016) 1617–1627.
[32] B. Hu, L. Yan, M. Shao, Adv. Mater. 21 (14–15) (2009) 1500–1516.
[33] Y.C. Hsiao, T. Wu, M. Li, B. Hu, Adv. Mater. 27 (18) (2015) 2899–2906.